High-resolution OCT balloon imaging catheter with astigmatism correction

Jiefeng Xi,[1,2] Li Huo,[1,2] Yicong Wu,[1,2] Michael J. Cobb,[1] Joo Ha Hwang,[3] and Xingde Li[1,2,*]

[1]*Department of Bioengineering, University of Washington, Seattle, Washington 98195, USA*
[2]*Current address: Department of Biomedical Engineering, Johns Hopkins University, Baltimore, Maryland 21205, USA*
[3]*Department of Medicine, Division of Gastroenterology, University of Washington, Seattle, Washington 98195, USA*
**Corresponding author: xingde@jhu.edu*

Received April 1, 2009; accepted April 24, 2009;
posted May 26, 2009 (Doc. ID 109597); published June 22, 2009

We report new optics designs for an optical coherence tomography (OCT) balloon imaging catheter to achieve diffraction-limited high resolution at a large working distance and enable the correction of severe astigmatism in the catheter. The designs employed a 1 mm diameter gradient-index lens of a properly chosen pitch number and a glass rod spacer to fully utilize the available NA of the miniature optics. Astigmatism caused by the balloon tubing was analyzed, and a method based on a cylindrical reflector was proposed and demonstrated to compensate the astigmatism. A catheter based on the new designs was successfully developed with a measured diffraction-limited lateral resolution of ~21 μm, a working distance of ~11–12 mm, and a round-shape beam profile. The performance of the OCT balloon catheter was demonstrated by 3D full-circumferential imaging of a swine esophagus *in vivo* along with a high-speed, Fourier-domain, mode-locked swept-source OCT system. © 2009 Optical Society of America

OCIS codes: 110.4500, 170.2150.

Many studies have shown that optical coherence tomography (OCT) can detect esophageal abnormalities, including Barrett's esophagus, subsquamous Barrett's esophagus, and neoplasia [1–5]. Miniature OCT fiber-optic catheters/endoscopes have been developed for enabling high-resolution *in vivo* OCT imaging of internal luminal organs, including the esophagus [6–10]. Most conventional OCT catheters have a high transverse resolution (e.g., 15–40 μm) and a short working distance (e.g., 1–3 mm). These catheters are well suited for imaging along a line or a small section of the esophagus when they are in direct contact with or close vicinity to the tissue surface. Recently, novel balloon imaging catheters have been developed to enable full-circumferential OCT imaging of the entire esophageal or colon lumen [11–13]. We previously demonstrated that a flexible and easy-to-implement catheter design based on microcompound lenses was able to achieve an excellent lateral resolution (e.g., ~35–40 μm) at a large and predictable working distance (e.g., 9–12 mm), while maintaining a small overall catheter diameter [11]; however, the resolution in the previous design was suboptimal. In addition, severe imaging beam distortion exists owing to the strong cylindrical lens effect of the balloon tubing. This cylindrical lens effect has been common in almost all side-viewing catheters where a transparent protective tube is used, yet this issue unfortunately has not been adequately addressed.

In this Letter, we present two new optics designs—a compound- and a single-lens configuration for balloon imaging catheters [see Figs. 1(A) and 1(B)], both of which can improve the resolution close to the diffraction limit without compromising the working distance or the overall optics diameter. We also analyze the beam distortion by the transparent tube and develop a practical and effective approach to correct such distortion. A new catheter based on the single-lens configuration with the distortion (or astigmatism) corrected was developed and its performance was demonstrated by real-time imaging of a pig esophagus *in vivo*.

For a gradient-index (GRIN) lens fiber-optic imaging probe, the ultimate resolution at a given working distance is controlled by the object distance (i.e., distance between the fiber tip to the GRIN lens) and the

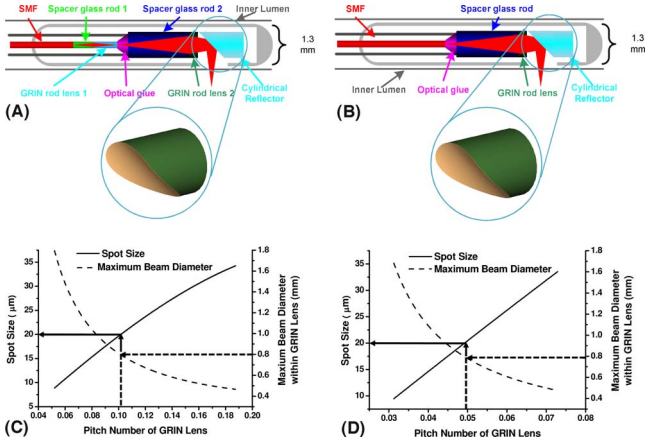

Fig. 1. (Color online) Catheter schematics of (A) a compound-lens configuration and (B) a single GRIN lens configuration. A cylindrical reflector [shown in the insets of (A) and (B)] is used to redirect the light by 90° and to correct the astigmatism caused by the inner balloon lumen. (C) and (D) are the calculated focused spot size and the maximum beam diameter within the GRIN lens versus the GRIN lens pitch number for the compound- and single-lens configurations, respectively. The target working distance was 10 mm in the calculation. The optimal pitch numbers, i.e., 0.1 and 0.05 for the compound- and single-lens configurations, respectively, are determined when the maximum beam diameter within the GRIN lens reaches 80% of the GRIN lens diameter, and the resultant finest resolution is ~20 μm.

pitch number of the GRIN lens (i.e., the focusing power). One practical factor is the beam diameter within the GRIN lens, which should be sufficiently small to avoid beam vignetting, and a consequent loss in transmission efficiency and degradation of the beam profile. Ray tracing analyses indicate that the maximum beam diameter within the GRIN lens is ~80% of the GRIN lens diameter to ensure a less than 5% transmission loss.

As mentioned above, the first configuration [see Fig. 1(A)] involves a compound lens (similar to the one reported previously [11]). In this configuration the tightly focused spot at the exit surface of the spot size reducer formed by the first glass rod and GRIN rod lens is relayed to a target working distance by a second glass rod spacer and a second GRIN lens of a larger diameter (i.e., 1.0 mm). To find the condition under which an optimal diffraction-limited resolution can be achieved for a target working distance (i.e., 10 mm), the focused beam spot size, the required length of the second glass spacer, and the maximum beam diameter within the second GRIN lens were calculated versus the pitch number of the second GRIN lens. Considering a 1 mm diameter GRIN lens, we find the optimal pitch number is ~0.1 (with a corresponding second glass spacer length of ~2.5 mm), under which the maximum beam diameter is not greater than 80% of the GRIN lens diameter and the finest focused spot size is ~20 μm [see Fig. 1(C)]. Similar analyses were performed for the second configuration, which involves a single GRIN lens [see Fig. 1(B)]. Different from the compound-lens configuration, light from a single-mode fiber (SMF) is directly focused by a spacer glass rod and a GRIN lens to the target working distance. As shown in Fig. 1(D), the finest resolution is again ~20 μm when using a GRIN lens of ~0.05 pitch (and a corresponding glass rod spacer of ~6.4 mm long), under which the available NA of the GRIN lens is fully utilized without beam vignetting. From an engineering standpoint, the single GRIN lens configuration is simple but requires accurate control of the short pitch for the GRIN lens.

In conventional side-viewing OCT catheters (including balloon imaging catheters), the beam is bent by 90° with a reflector and then passes through a transparent plastic protective tube. The tube, however, acts as a negative cylindrical lens, which diverges the beam along the azimuthal direction perpendicular to the longitudinal axis of the catheter [14]. This common effect has not been systematically addressed. The degradation of the beam can often be severe, in particular when the transparent tube has a small radius and a relatively thick wall. For the inner tube used in our balloon catheter, which has a 0.7 mm radius and an ~190 μm wall thickness, the calculated ratio of the beam spot size in the azimuthal direction to the one in the longitudinal direction (defined as the astigmatism ratio) is ~40 [see Fig. 2(A)], which was observed on the beam profile photograph captured on the target focus plane [as shown in Fig. 2(C)]. To compensate for the astigmatism, the beam needs to be refocused along the azimuthal direction.

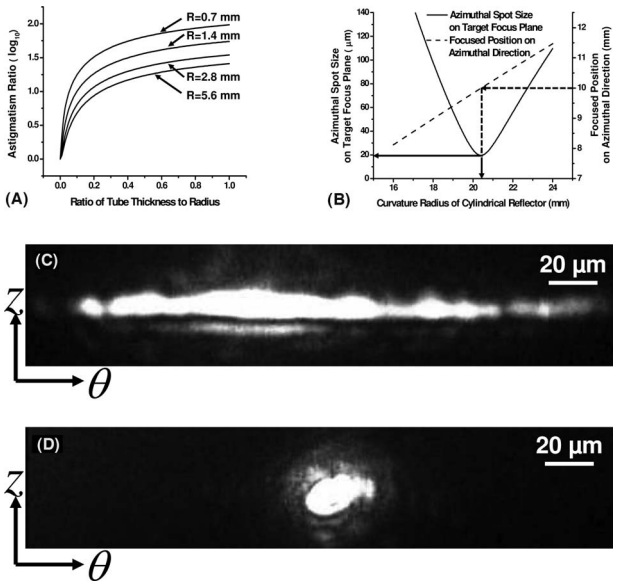

Fig. 2. (A) Logarithm of the calculated astigmatism ratio versus the ratio of the tube thickness ΔR to tube radius for several tube radii R. The results show that the beam profile distortion increases with the ratio of $\Delta R/R$, and the distortion becomes more severe for a tube of a smaller radius. (B) Calculated beam spot size in the azimuthal direction on the target focus plane (i.e., 10 mm away from the GRIN lens and perpendicular to the beam axis) and the actual focused position on the azimuthal direction versus the curvature radius of the astigmatism-correcting cylindrical reflector. Simulation shows that a cylindrical reflector with an ~20.5 mm radius could refocus the beam back to the target working distance. (C) Photograph of the beam profile on the target focal plane when a conventional flat reflector was used in the catheter, where severe distortion was evident. (D) Photograph of the beam profile when a cylindrical concave reflector of an ~20.5 mm radius was used, where an approximately circular beam profile was restored.

One solution is to replace the commonly used flat reflector with a cylindrical reflector. Our numerical simulations show that a cylindrical reflector with an ~20.5 mm radius of curvature would fully compensate for the cylindrical effect caused by the inner lumen in our balloon catheter [see Fig. 2(B)].

It is straightforward to construct a balloon imaging catheter once the above parameters are determined, including the pitch number of the GRIN lens, the glass rod spacer length, and the curvature of the cylindrical reflector. Here, we will only describe the engineering details for the single-lens design owing to its engineering simplicity. A commercially available 1 mm diameter GRIN lens was first cut and polished down to ~0.05 pitch (i.e., ~0.52 mm long). The length of the glass rod spacer required to focus the beam to the target 10 mm working distance was ~6.36 mm to achieve a diffraction-limited resolution (e.g., ~20 μm) without beam vignetting [see Fig. 1(D)]. The spacer rod and the GRIN lens were then UV glued together. The actual spot size and working distance were fine-tuned by adjusting the gap between the SMF and the spacer-lens unit during the catheter assembling process. The distal end optics including the SMF and the spacer-lens unit were then UV glued together and housed in a protective metal

tube with a precut window for the beam to pass through. A custom-polished cylindrical aluminum reflector with the required radius of curvature (~20.5 mm), and a measured reflectivity of ~86% at 1300 nm was placed at the end of the catheter (within the metal tube) to redirect the beam by ~90° and to compensate the cylindrical effect caused by the balloon's inner lumen. The measured spot size and the working distance of the catheter were 21.2 μm and 11.2 mm, respectively, which are very close to the predicted resolution limit (e.g., 21.0 μm at a working distance of 11.2 mm). The beam profiles before and after the correction of the cylindrical effect are shown, respectively, in Figs. 2(C) and 2(D), which clearly demonstrate that the proposed approach can effectively correct the astigmatism and restore the round shape of the beam profile.

The performance of the high-resolution balloon imaging catheter was tested for 3D imaging of the esophagus in a swine model *in vivo*. Real-time imaging was conducted using a Fourier-domain, mode-locked (FDML) swept-source OCT (SS-OCT) system [15]. It operated at 1300 nm center wavelength, with a 3 dB spectral bandwidth of ~103 nm and a sweeping rate of 40 kHz. At 40 kHz sweeping rate, full-circumferential images were acquired, processed, displayed, and saved in real time at 10 frames/s with each frame consisting of 2048×4000 pixels (axial ×circumferential) where only forward scans were used. The measured resolution of the imaging system was 10.2 μm (axial resolution in air) and 21.2 μm (circumferential) with a detection sensitivity of ~120 dB. A representative 2D OCT snapshot of a swine esophagus *in vivo* is displayed in Fig. 3(A) where the normal layered esophageal structures can be clearly identified. A cutaway 3D image reconstructed from a series of 2D images 20 μm apart is shown in Fig. 3(B). It is noted that eccentricity between the inner and outer balloon lumens degrades imaging quality. This issue can potentially be solved by choosing the right inner lumen material and rigidity.

In summary, we developed two new designs for an OCT balloon imaging catheter based on compound- and single-lens configurations. These designs improve the lateral resolution by a factor of 2 compared with the previous design while maintaining a large working distance. In addition, the severe astigmatism induced by the transparent inner lumen in the balloon was also analyzed and compensated by introducing a cylindrical reflector with a proper radius of curvature. An *in vivo* animal model study was performed and the result suggests the potential of an OCT balloon imaging catheter for systematic imaging surveillance of the human esophagus in clinic.

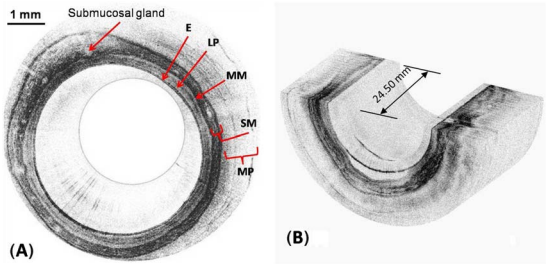

Fig. 3. (Color online) Representative real-time OCT images of a pig esophagus *in vivo* acquired with the balloon imaging catheter in conjunction with an FDML SS-OCT system. (A) 2D snapshot and (B) 3D cutaway view. Different stratified layers of the esophagus can be clearly identified, including epithelium (E), lamina propria (LP), muscularis mucosae (SM), submucosae (SM), muscularis propria (MP), and the submucosal gland as labeled in (A).

The authors are grateful to Jeff Magula for his assistance with the imaging system and Cindy Warren for her assistance with tissue collection and the *in vivo* experiments. This work was supported in part by the National Institutes of Health (NIH) (contracts R21 CA116442 and R01 CA120480). X. D. Li acknowledges support from the National Science Foundation (NSF) Career Award. X. D. Li and J. H. Hwang acknowledge support from Coulter Foundation Translational Research Awards.

References

1. B. E. Bouma, G. J. Tearney, C. C. Compton, and N. S. Nishioka, Gastrointest. Endosc. **51**, 467 (2000).
2. M. V. Sivak, Jr., K. Kobayashi, J. A. Izatt, A. M. Rollins, R. Ung-runyawee, A. Chak, R. C. K. Wong, G. A. Isenberg, and J. Willis, Gastrointest. Endosc. **51**, 474 (2000).
3. X. D. Li, S. A. Boppart, J. Van Dam, H. Mashimo, M. Mutinga, W. Drexler, M. Klein, C. Pitris, M. L. Krinsky, M. E. Brezinski, and J. G. Fujimoto, Endoscopy **32**, 921 (2000).
4. G. Isenberg, M. V. Sivak, A. Chak, R. C. K. Wong, J. E. Willis, B. Wolf, D. Y. Rowland, A. Das, and A. Rollins, Gastrointest. Endosc. **62**, 825 (2005).
5. M. J. Cobb, M. P. Upton, Y. Chen, D. J. MacDonald, J. H. Hwang, M. B. Kimmey, and X. D. Li, in *Biomedical Optics*, OSA Technical Digest (CD) (Optical Society of America, 2006), paper TuI26.
6. G. J. Tearney, S. A. Boppart, B. E. Bouma, M. E. Brezinski, N. J. Weissman, J. F. Southern, and J. G. Fujimoto, Opt. Lett. **21**, 912 (1996).
7. A. M. Rollins, R. Ung-arunyawee, A. Chak, R. C. K. Wong, K. Kobayashi, M. V. Sivak, and J. A. Izatt, Opt. Lett. **24**, 1358 (1999).
8. X. M. Liu, M. J. Cobb, Y. C. Chen, M. B. Kimmey, and X. D. Li, Opt. Lett. **29**, 1763 (2004).
9. A. R. Tumlinson, B. Povazay, L. P. Hariri, J. McNally, A. Unterhuber, B. Hermann, H. Sattmann, W. Drexler, and J. K. Barton, J. Biomed. Opt. **11**, 064003 (2006).
10. D. L. Wang, B. V. Hunter, M. J. Cobb, and X. D. Li, IEEE J. Sel. Top. Quantum Electron. **13**, 1596 (2007).
11. H. L. Fu, Y. Leng, M. J. Cobb, K. Hsu, J. H. Hwang, and X. D. Li, J. Biomed. Opt. **13**, 060502 (2008).
12. M. J. Suter, B. J. Vakoc, P. S. Yachimski, M. Shishkov, G. Y. Lauwers, M. Mino-Kenudson, B. E. Bouma, N. S. Nishioka, and G. J. Tearney, Gastrointest. Endosc. **68**, 745 (2008).
13. D. C. Adler, C. Zhou, T.-H. Tsai, J. Schmitt, Q. Huang, H. Mashimo, and J. G. Fujimoto, Opt. Express **17**, 784 (2009).
14. A. R. Tumlinson, L. P. Hariri, U. Utzinger, and J. K. Barton, Appl. Opt. **43**, 113 (2004).
15. R. Huber, M. Wojtkowski, and J. G. Fujimoto, Opt. Express **14**, 3225 (2006).